

# Real-time mapping of a hydrogen peroxide concentration profile across a polymicrobial bacterial biofilm using scanning electrochemical microscopy

Xiuhui Liu<sup>a</sup>, Matthew M. Ramsey<sup>b</sup>, Xiaole Chen<sup>a</sup>, Dipankar Koley<sup>a</sup>, Marvin Whiteley<sup>b</sup>, and Allen J. Bard<sup>a,1</sup>

<sup>a</sup>Center for Electrochemistry, Department of Chemistry and Biochemistry, University of Texas at Austin, 1 University Station A5300, Austin, TX 78712-0165; and <sup>b</sup>Section of Molecular Genetics and Microbiology, University of Texas, Austin, TX 78712

Contributed by Allen J. Bard, December 10, 2010 (sent for review September 29, 2010)

**Quantitative detection of hydrogen peroxide in solution above a *Streptococcus gordonii* (*Sg*) bacterial biofilm was studied in real time by scanning electrochemical microscopy (SECM). The concentration of hydrogen peroxide was determined to be 0.7 mM to 1.6 mM in the presence of 10 mM glucose over a period of 2 to 8 h. The hydrogen peroxide production measured was higher near the biofilm surface in comparison to *Sg* grown planktonically. Differential hydrogen peroxide production was observed both by fluorometric as well as by SECM measurements. The interaction between two different species in a bacterial biofilm of *Sg* and *Aggregatibacter actinomycetemcomitans* (*Aa*) in terms of hydrogen peroxide production was also studied by SECM. One-directional y-scan SECM measurements showed the unique spatial mapping of hydrogen peroxide concentration across a mixed species biofilm and revealed that hydrogen peroxide concentration varies greatly dependent upon local species composition.**

real-time (detection) | metabolite efflux | local concentration | oral flora | Au UME

*Streptococcus gordonii* (*Sg*) is a member of the viridans group streptococci—Gram-positive oral microbes that are known to ferment sugars into lactic acid and produce hydrogen peroxide in the presence of oxygen (1). The presence of these beneficial oral streptococci has been shown to improve oral health, by either competition with pathogens for nutrients in the oral cavity or by the production of inhibitory concentrations of hydrogen peroxide. Populations of viridans group streptococci negatively correlate with the presence of many notable oral pathogens (2, 3). However, recent work has demonstrated that in vitro *Sg* can grow in coculture with the opportunistic oral pathogen *Aggregatibacter actinomycetemcomitans* (*Aa*) (4). In co-culture *Aa* preferentially utilizes *Sg*-produced lactic acid (5) and detoxifies *Sg*-produced hydrogen peroxide using the KatA enzyme (6). Recent work has demonstrated that hydrogen peroxide induces katA expression as well as *apiA*, which encodes an immunoprotective factor that renders *Aa* more resistant to killing by host innate immunity (5). These studies demonstrated induction of gene expression in mixed species biofilms by *Sg*-produced hydrogen peroxide. Because hydrogen peroxide is rapidly degraded by catalase and can also react with other biological materials, we sought to quantify local hydrogen peroxide concentrations in real time to be utilized for future polymicrobial experiments between *Sg*, *Aa*, and other oral bacteria.

Previous measurements of hydrogen peroxide have been performed using fluorescence, spectroscopy and other methods (1, 7–10). However, current techniques lack the ability to quantify local hydrogen peroxide concentrations at the surface of a biofilm. In this study, scanning electrochemical microscopy (SECM) was used to address this problem. SECM has the unique ability to set the exact distance from a sensing tip [an ultramicroelectrode (UME) of size ~10 to 25  $\mu\text{m}$  diameter] to a substrate through a feedback approach curve (11) (tip current,  $i_T$ , vs. distance above substrate,  $d$ ) and thus is able to measure the local concentration

over a biofilm. Several studies concerned with the electrochemical measurement of hydrogen peroxide concentration have been reported (12–17), but none dealt with spatial mapping adjacent to a biofilm surface. In addition, SECM has the ability to scan over a substrate in the  $x$ - $y$  direction and thus is able to record a unique spatial concentration profile over the surface. SECM has been used before in biological systems (18–24) to measure the local concentration over soft biological samples and for imaging. SECM is thus a new analytical tool to study not only the local hydrogen peroxide concentration in a bacterial biofilm but also to map the hydrogen peroxide concentration spatially across two different species of bacteria located distally in a biofilm. This allows the determination of the actual hydrogen concentration produced by *Sg* and the quantification of the effective hydrogen peroxide concentration encountered by a neighboring organism such as *Aa*. This introduces SECM for use in such real-time mapping of local hydrogen peroxide concentration in a biofilm and determination of the consumption of hydrogen peroxide in a polymicrobial biofilm during spatial scanning. This allows us to measure the effective concentration of hydrogen peroxide in situ, the flux of hydrogen peroxide at the bacterial surface, and determine how it might shape polymicrobial interactions.

## Results

**Real-Time Quantitative Measurement of Hydrogen Peroxide Produced by Living *Sg* Colony Biofilms with SECM.** Fig. 1*D* shows the formation of hydrogen peroxide by a *Sg* colony biofilm (25) as a function of time (min) at 100  $\mu\text{m}$  and 200  $\mu\text{m}$ , respectively, above the film. Each concentration point in the plot corresponds to the chronoamperometric current due to hydrogen peroxide oxidation at a particular time, e.g.,  $t = 30$  min. The concentration was calculated from the current recorded at 10 s using the calibration curve shown in Fig. S1.

For a pure *Sg* biofilm with the tip 100  $\mu\text{m}$  away, the hydrogen peroxide concentration increased initially for about 10 to 12 min and then tended to a quasi-steady-state concentration of approximately 1.4 mM. This behavior can be understood in terms of a substrate, the biofilm, with a sufficiently large area that diffusion from it can be considered linear. However, as is well known from the behavior of electrodes generating a species with a constant flux, diffusional behavior can only be maintained, even with careful isolation of the cell from vibrations, for a time of 5 to 10 min. At some stage natural convection begins and the current then tends to a steady-state governed by the convection rate (26). When the tip was placed at 200  $\mu\text{m}$  above the membrane for the

Author contributions: M.W. and A.J.B. designed research; X.L., M.M.R., and X.C. performed research; D.K. carried out simulations; and X.L., M.M.R., X.C., D.K., M.W., and A.J.B. wrote the paper.

The authors declare no conflict of interest.

<sup>1</sup>To whom correspondence should be addressed. Email: ajbard@mail.utexas.edu.

This article contains supporting information online at [www.pnas.org/lookup/suppl/doi:10.1073/pnas.1018391108/-DCSupplemental](http://www.pnas.org/lookup/suppl/doi:10.1073/pnas.1018391108/-DCSupplemental).



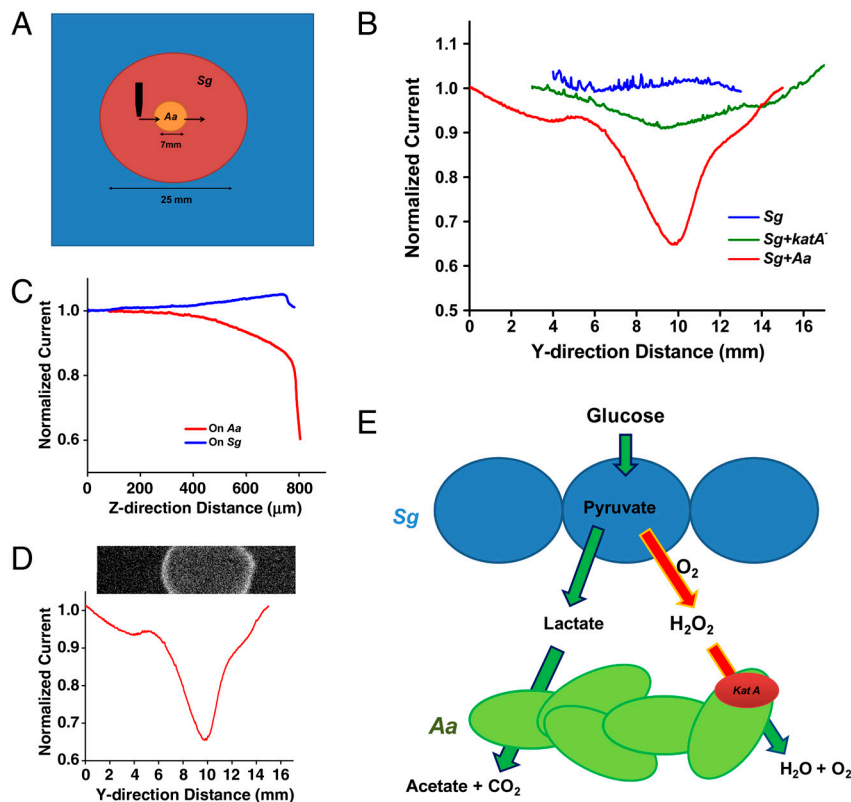


**Fig. 2.** (A) Schematic diagram of tip scan across the region of a mixed species biofilm in the order of *Sg*-*Aa*-*Sg*. (B) Normalized current changes of an SECM y-scan over *Sg* alone, mutant *Aa* in an *Sg* film, and wild-type *Aa* in an *Sg* film, respectively, at 37 °C. Tip potential was held at 0.8 V, and scan rate was 150 μm/s. Green is pure *Sg*, blue is mutant *Aa* with *Sg*, red is wild *Aa* with *Sg*. (C) Approach curves for pure *Sg* and wild-type *Aa* region in an *Aa* + *Sg* biofilm (B, red curve). (D) Normalized current changes of an SECM y-scan over *Aa* + *Sg* biofilm extrapolated to identical biofilms using *Aa* carrying the *katA-lux* reporter vector. Light production (in white) is indicative of promoter response to hydrogen peroxide. (E) Model for the role of hydrogen peroxide in an *Sg* and *Aa* cocultured biofilm.

(Fig. 2B, red curve), however, showed an evident current decrease (valley) over the *Aa* region on the membrane. The width of the valley was about 7,000 μm, consistent with the diameter of the *Aa* spot made on the *Sg* biofilm (seen in Fig. 2D). The current in the valley dropped to approximately 0.66 of the current for the *Sg* region. The blue curve in Fig. 2B displays the y-scan over the *Aa katA*-mutant doped *Sg* biofilm. It shows a slight current dip over the *Aa katA*-mutant region as well; here the current dropped only to approximately 0.91 compared to *Sg*, indicating that a higher concentration of hydrogen peroxide is observed on the *Aa* mutant lacking catalase (*katA*) compared to wild-type *Aa*.

Approach curves were collected over the pure *Sg* region ( $y = 1,000 \mu\text{m}$ ) and the *Aa* region ( $y = 10,000 \mu\text{m}$ ) in the same membrane, respectively (see Fig. 2C). The approach curve over the *Sg* region showed a steady current increase as the tip approached the *Sg* membrane over a distance of 300 μm, indicating that a higher concentration of hydrogen peroxide was found near the *Sg* membrane. Over the *Aa* region, however, a current drop was observed as the tip moved closer to the *Aa* surface, showing a negative deviation from the usual negative feedback mode approach curve as a result of shielding because of consumption of hydrogen peroxide in the *Aa* region.

## Discussion

**Real-Time Quantitative Measurement of Local Hydrogen Peroxide Concentration Produced by a *Sg* Biofilm.** *Sg*-produced hydrogen peroxide was measured with a SECM tip located approximately 100 to 200 μm above the biofilm in the experimental setup as shown in Fig. 1A and B. The biofilm itself was 10 to 20 μm thick as measured by confocal laser scanning microscopy (SI Text). Although individual measurements were expected to be different because

of biological variability (e.g., cell condition, number of the bacterial cells on the membrane), most concentration vs. time profiles we observed were very similar in shape to that shown in Fig. 1D. A quasi steady-state hydrogen peroxide concentration of 1.4 mM was observed (Fig. 1D, curve b) at 100 μm away from biofilm, while only 0.4 mM hydrogen peroxide was recorded at 200 μm over 60 min in the presence of 10 mM glucose as shown in Fig. 1D, curve a. As indicated earlier, this difference in hydrogen peroxide measurement may be due to mass transfer of hydrogen peroxide produced by the biofilm into the bulk phase by natural and induced convection. In addition, a slower response of hydrogen peroxide above the biofilm is observed at 200 μm because it takes a much longer time to build up detectable hydrogen peroxide concentrations at this distance through diffusion and convection. This is supported by Fig. 1E, where a higher hydrogen peroxide concentration (1.6 mM) is observed at 200 μm away for the same type of *Sg* biofilm when exposed to 10 mM glucose for 8 h.

Fig. 3 shows the fitted simulated curve demonstrating diffusion of hydrogen peroxide from the film to the SECM tip could be fit to the experimental response by the biofilm upon exposure to 10 mM glucose. The simulated curve (the solid line) fit the experimental data (dots) for about 10 min and then began to deviate because of the onset of natural convection during measurement (not considered in the simulation model). However, the response for the first 10 min could be used to predict the flux at the biofilm surface. As discussed previously, SECM was a very useful tool in measuring the local concentration of peroxide above the biofilm or 100 μm from the biofilm surface, it still did not give the concentration or flux at the biofilm surface. With the aid of digital simulation, the exact hydrogen peroxide flux at

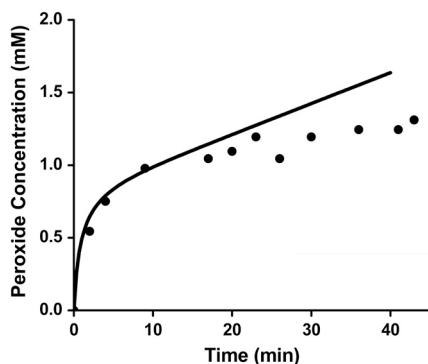


**Fig. 3.** The simulated (solid line) hydrogen peroxide metabolite efflux from bacterial biofilm of *Sg* at a distance of 100  $\mu\text{m}$  from surface compared to experimental measurements (dots). The diameter of the SECM tip used was 25  $\mu\text{m}$  (RG = 10).

the biofilm surface can be calculated as in SECM experiments, when the tip-substrate distance is known. The details of the simulation model can be found in *SI Text*. Briefly, the simulation assumes only diffusional mass transfer and a constant hydrogen peroxide flux from the biofilm surface to a 25  $\mu\text{m}$  SECM tip (RG = 10) at a distance of 100  $\mu\text{m}$  away from the surface. The fitted hydrogen peroxide flux at the biofilm surface was determined to be  $1.0 \times 10^{-11}$  mol/cm<sup>2</sup>/s. Assuming a dimension of each bacterium is 1.5  $\mu\text{m} \times 0.8 \mu\text{m}$ , the calculated bacterial density was  $8.3 \times 10^7$ /cm<sup>2</sup>. So, approximately  $1.2 \times 10^{-19}$  mol (~70,000 molecules) of hydrogen peroxide effluxed from a single bacterium at the film surface per second. This gives an important estimate of the amount of hydrogen peroxide produced at the bacteria surface, which may be useful for elucidating the defense mechanism of a bacterial species or interactions with other bacterial species in terms of metabolite or hydrogen peroxide concentration.

Interestingly, significantly lower concentrations (20–40  $\mu\text{M}$  range) of hydrogen peroxide are observed in Table 1 both for biofilm as well as cell suspensions when measured by taking aliquots of bulk solution using a commercial fluorometric assay. Similar bacterial numbers and incubation times in 1.5 mL of chemically defined medium (CDM) culture solution were used for the same time periods in both methods for comparison. Results suggest that the local hydrogen peroxide concentration is significantly higher for a biofilm in comparison to the bulk phase and that SECM is an ideal analytical tool due to its ability to measure such concentrations close to the biofilm surface. However, it is difficult to understand the results in terms of diffusion from the bacteria surface at times longer than about 10 min at most.

It is also important to carefully consider the conditions at which the metabolite concentration measurements are made before considering any of their effects on bacterial functions or their interactions with other bacterial species; especially for toxic molecules such as hydrogen peroxide. As observed from our SECM experiments, the *Sg* biofilm is able to produce sufficient hydrogen peroxide (mM range) to inhibit the growth of

**Table 1. Comparison of hydrogen peroxide production concentration from *Sg* by fluorometric and electrochemical measurement**

H <sub>2</sub> O <sub>2</sub> concentration at different experimental setup	Time (h)		
	2	4	8
Suspension fluorometric measurement	19.2 $\mu\text{M}$	20.2 $\mu\text{M}$	30.6 $\mu\text{M}$
Biofilm fluorometric measurement	21.0 $\mu\text{M}$	19.0 $\mu\text{M}$	30.6 $\mu\text{M}$
Biofilm electrochemical measurement (at 200 $\mu\text{m}$ away)	0.7 mM	0.9 mM	1.6 mM

many bacteria, but such conditions prevail only at a very close distance from the biofilm surface. The presence of higher hydrogen peroxide concentrations close to the surface (~200  $\mu\text{m}$ ) is also observed in the hydrogen peroxide approach curve (shown in Fig. 1*F*). The sharp drop in current or hydrogen peroxide concentration happens when the tip touches the surface and thus blocks any further diffusion of hydrogen peroxide to the tip. Fluorescent dyes are available to detect reactive oxygen species such as hydrogen peroxide and superoxides in individual cells; however, such techniques only provide qualitative information about these metabolites. Thus, SECM has a significant advantage in measuring local concentrations spatially across a biofilm to elucidate how mass transfer affects this complex and dynamic biological system; existing biological analytical methods are unable to obtain such information.

**KatA Mediated Decomposition of Hydrogen Peroxide in a Mixed Species Biofilm.** The y-direction SECM scan shown in Fig. 2*B* (red curve) over cocultured *Sg* and *Aa* wild-type biofilms reveals a unique hydrogen peroxide concentration profile across two different regions. The current from hydrogen peroxide oxidation at the tip while scanning over the *Aa* region exhibits a lower concentration (~34% decrease) based on the normalized currents at the deepest point, indicating that hydrogen peroxide is consumed by *Aa*. The reason for this consumption can be explained as shown in the model in Fig. 2*E*. According to the proposed model (4), wild-type *Sg* bacteria can produce hydrogen peroxide by metabolizing glucose in the presence of oxygen. *Aa* is able to flourish in this environment by decomposing hydrogen peroxide using the KatA enzyme. This model has been validated in our experiments by performing y-scans over *Aa katA*<sup>-</sup>, which is unable to detoxify hydrogen peroxide in the presence of *Sg*. As shown in Fig. 2*B* (blue curve), no significant decrease in y-scan current or concentration is noticed, thus confirming no hydrogen peroxide consumption by *Aa katA*<sup>-</sup>. The slight dip in y-scan current over the mutant *Aa* zone is, however, due to lower hydrogen peroxide concentration over a void space created by the nonconsuming and non-hydrogen-peroxide-producing mutant *Aa*. Because the *Aa* spot is surrounded by hydrogen peroxide producing *Sg* bacteria (Fig. 2*A*), hydrogen peroxide can diffuse from the surrounding area and subsequently fill the empty *Aa* spot. No dip in current is observed in Fig. 2*B* (green curve) when the tip is scanned over the *Sg*-only bacterial biofilm because no spatial change in hydrogen peroxide concentration in the y-direction is expected at a given height.

## Materials and Methods

**Chemicals.** Sulfuric acid (94–98%, trace metal grade), potassium nitrate, potassium chloride, agar purified grade, and o-phosphoric acid (85%) from Fisher Scientific were used as received. Fresh solutions of hydrogen peroxide were made before each experiment by diluting a concentrated commercial aqueous solution (30% (v/v), Sigma-Aldrich GmbH). All solutions were prepared with deionized Milli-Q water.

**Bacterial Strains Culture and Preparation.** *Streptococcus gordonii* strain DL1, *Aggregatibacter actinomycetemcomitans* Y4 and *Aa* Y4 *katA*<sup>-</sup> containing an insertion mutant of the catalase-encoding gene *katA* (6) were used in our study. Broth cultures were grown by shaking at 150 RPM at 37 °C in a 5% CO<sub>2</sub> atmosphere unless specified otherwise. The growth medium included Tryptic soy broth +5% yeast extract (TSBYE) or CDM (5).

*Sg* was inoculated from a single colony into 3 mL TSBYE broth and grown overnight to an approximate cell density of  $3 \times 10^9$  cells/mL ( $A_{600} = 3$ ). Cells were next diluted into 3 mL of TSBYE to a density of  $A_{600} = 0.05$  and grown to a density of  $A_{600} = 0.5$ . 2 mL of cells were collected via centrifugation at  $10,000 \times g$  for 5 min and resuspended in 1 mL phosphate buffered saline (PBS). 25 mm polycarbonate membranes (Whatman, 0.2  $\mu\text{m}$  pore size) were aseptically transferred to the surface of a 100 mm TSAYE agar plate. 50  $\mu\text{L}$  of the above cell suspension ( $\sim 5 \times 10^7$  cells) was spotted directly onto the membrane surface and uniformly spread to cover the entire membrane using a sterile spreader. Cell suspensions were dried on the membranes

for approximately 10 min in a laminar flow hood to form a colony biofilm. TSAYE plates and membranes containing bacterial biofilm were transferred back to 37 °C and 5% CO<sub>2</sub> environment for approximately 1 h.

*Aa* strains were grown overnight in 3 mL TSBYE to a cell density of  $A_{600} = 1$ ; then diluted into 3 mL of TSBYE to a density of  $A_{600} = 0.05$ . Cells were then grown to a density of  $A_{600} = 0.5$  and 2 mL were centrifuged as above and resuspended in 1 mL of PBS. Cells were then diluted 1:10 in PBS buffer. 5  $\mu$ L of cell suspension (corresponding to  $\sim 5 \times 10^6$ ) cells were spotted directly on the center of the *Sg* coated membrane prepared as above prior to the final 1 h incubation step at 37 °C. The polycarbonate membrane, as a result, had 25 mm bacterial biofilm of *Sg* with a spot of 5 to 7 mm *Aa* in the middle. Biofilm preparations with the *katA*- mutant were performed identically.

**Ultramicroelectrode Fabrication.** Gold (99.99 + %) wire, 25  $\mu$ m diameter, from Goodfellow was used to fabricate the SECM tip. First it was fabricated by heat sealing the corresponding metal wire under vacuum in a borosilicate glass capillary. Then it was polished and shaped conically by a wheel with 180-grid Carbimet paper disks and micropolishing cloth with 1.0, 0.3, and 0.05  $\mu$ m alumina. The tip used in this study was sharpened to  $RG = 2$ , where  $RG$  is the ratio between the radius of the glass sheath and the radius of the active electrode surface. Before each experiment, the Au tip was polished with alumina paste (0.3 and 0.05  $\mu$ m) on microcloth pads (Buehler), sonicated for 15 min in water, and then electrochemically cleaned by cycling between 0.2 and 1.4 V in 0.1 M sulfuric acid for 40 cycles to a constant CV. 0.5 mm tungsten wire from Alfa Products was used as an auxiliary electrode. Ag|AgCl|3 M KCl was used as reference electrode to which all potentials for electrochemical experiments are referred.

**Real-Time Electrochemical Monitoring of Hydrogen Peroxide by SECM on a *Sg* Biofilm.** An *Sg*-coated 25 mm polycarbonate membrane was prepared as described in *Bacterial Strains Culture and Preparation*. The membrane was then transferred carefully from the agar plate onto a piece of double sided tape (3M: 34-8517-3569-5) fixed to the bottom of a 35 mm Petri dish (Becton Dickinson). The dish was later put on a home built copper heating plate on the CHI 920C SECM stage (CHI Instruments) to maintain a constant temperature of 37 °C. The experimental setup for SECM measurements is shown in Fig. 1 A and B. The biofilm was incubated for 1 h at 37 °C after adding 1.5 mL of CDM solution to the 35 mm Petri dish. During this period, an approach curve (tip current,  $i_T$ , vs. distance,  $d$ ) was taken over the biofilm with oxygen as a mediator by holding the tip at  $-0.6$  V (seen in Fig. 1C). Tip-membrane distance was then fixed at 200  $\mu$ m. The background was recorded at the same height by pulsing the tip from 0.55 to 0.80 V for 10 s. 15  $\mu$ L of 1 M of glucose was added to the existing 1.5 mL of CDM buffer to make the final glucose concentration 10 mM. The hydrogen peroxide concentration over the biofilm was measured as a function of time by pulsing the tip at the same potential range of background recording every 5 min.

**Y-scan and Approach Curve SECM Experiment on a *Sg* and *Aa* Coculture Biofilm.** The biofilm sample was prepared by the same method as described in *Bacterial Strains Culture and Preparation*. The only difference in this sample was a 5 to 7 mm diameter spot of *Aa* in the middle of the *Sg* biofilm. As shown in Fig. 2A, the location of the *Aa* spot was marked on the outside of the Petri dish with a marker. The same SECM imaging procedure was followed as before with the tip-substrate distance at 200  $\mu$ m and the background current recorded at the same height. First, the growth of the hydrogen peroxide concentration was observed at  $d = 200$   $\mu$ m over the *Sg* area for 1 h. The tip was then scanned at 150  $\mu$ m/s in the  $y$ -direction at  $d = 200$   $\mu$ m from *Sg*-*Aa*-*Sg* to record the hydrogen peroxide concentration across the two

different bacterial populations. Approach curves were performed using hydrogen peroxide as a mediator at three different points: one on *Sg* and one on *Aa* and another one again on *Sg*.

**Fluorometric Measurements of Hydrogen Peroxide.** Hydrogen peroxide production was measured using the Amplex Red hydrogen peroxide assay kit (Invitrogen) using the manufacturer protocols. *Sg* was cultured as mentioned above and  $5 \times 10^7$  cells were either spread onto a 25 mm polycarbonate membrane to form a biofilm and then placed in a 35 mm Petri dish or resuspended directly in 1.5 mL of CDM + 10 mM glucose. Biofilm cells were covered with 1.5 mL CDM + 10 mM glucose. Aliquots were taken from each culture in triplicate at 2, 4, and 8 h then measured using the above assay kit on a BioTek Synergy MX (BioTek) fluorometric microplate reader at excitation/emission values of 530 nm and 590 nm, respectively. For *lux* reporter experiments we used the *Aa katA-lux* reporter strain (4) in place of *Aa* WT in the biofilm overlay. *Aa katA-lux* was grown to the exponential phase and  $5 \times 10^8$  cells were isolated via centrifugation at  $10,000 \times g$  for 10 min. Cells were resuspended in 5  $\mu$ L TSBYE and placed onto the surface of the *Sg* biofilm prepared as above. Biofilms were incubated on the surface of a TSAYE plate at 37 °C for approximately 1 h, then image captures were exposed for 10 min in a Syngene G:BOX (Syngene) using the manufacturers software. Image sizes were scaled to the  $x$ -axis using Photoshop CS5 (4).

**Simulations.** Simulations were performed with Comsol Multiphysics 3.3 on a 2.8 GHz Intel Pentium IV processor and 2 GB RAM desktop PC. Details about the simulation model are given in *SI Text*.

## Conclusions

By using SECM, we measured the local hydrogen peroxide concentration produced by *Sg* biofilms in real time and found it to be significantly different than suspension hydrogen peroxide measurements. The concentration of hydrogen peroxide can reach 1.2 mM with the tip placed 100  $\mu$ m away from the biofilm. A quasi-steady-state concentration was always observed, as hydrogen peroxide is likely decomposed by *Sg* to prevent injury by excessive hydrogen peroxide concentrations. Furthermore, we also measured local hydrogen peroxide concentrations across *Sg* and *Aa* cocultured biofilms with a one-directional scan SECM technique. Our results confirmed not only that *Aa* catalase activity was critical for decreasing local hydrogen peroxide concentration but also that this decomposition effect was only observed in the immediate vicinity of *Aa*. Quantitative investigation with these and other bacteria will help us to understand the mechanism of how hydrogen peroxide influences the ecology of mixed species communities.

**ACKNOWLEDGMENTS.** A.J.B. acknowledges support from the Robert A. Welch Foundation (F-0021) and the National Science Foundation (CHE-0808927). X.L. thanks the Natural Science Foundation of China (Grant 20875077), the National Scholarship Fund of China Scholarship Council ([2007]3045), Key Laboratory of Bioelectrochemistry & Environmental Analysis of Gansu Province, and the Key Laboratory of Polymer Materials of Gansu Province for support. Fu-Ren F. Fan is also gratefully acknowledged for helpful discussions. M.W. and M.M.R. thank the National Institutes of Health (5R01AI075068 to M.W. and 5F31DE019995 to M.W. and M.M.R.) for support. M.W. is a Burroughs Wellcome Investigator in the Pathogenesis of Infectious Disease.

1. Barnard JP, Stinson MW (1999) Influence of environmental conditions on hydrogen peroxide formation by *Streptococcus gordonii*. *Infect Immun* 67:6558–6564.
2. De Stoppelaar JD, et al. (1969) The relationship between extracellular polysaccharide-producing streptococci and smooth surface caries in 13-year-old children. *Caries Res* 3:190–199.
3. Kreth J, et al. (2008) Streptococcal antagonism in oral biofilms: *Streptococcus sanguinis* and *Streptococcus gordonii* interference with *Streptococcus mutans*. *J Bacteriol* 190:4632–4640.
4. Ramsey MM, Whiteley M (2009) Polymicrobial interactions stimulate resistance to host innate immunity through metabolite perception. *Proc Natl Acad Sci USA* 106:1578–1583.
5. Brown SA, Whiteley M (2007) A novel exclusion mechanism for carbon resource partitioning in Aggregatibacter actinomycetemcomitans. *J Bacteriol* 189:6407–6414.
6. Thomson VJ, et al. (1999) Direct selection of IS903 transposon insertions by use of a broad-host-range vector: Isolation of catalase-deficient mutants of *Actinobacillus actinomycetemcomitans*. *J Bacteriol* 181:7298–307.
7. Jakubovics NS, Gill SR, Vickerman MM, Kolenbrander PE (2008) Role of hydrogen peroxide in competition and cooperation between *Streptococcus gordonii* and *Actinomyces naeslundii*. *FEMS Microbiol Ecol* 66:637–644.
8. Mendoza AG, Liébana J, Castillo AM, de la Higuera A, Piédrola G (1993) Evaluation of the capacity of oral streptococci to produce hydrogen peroxide. *J Med Microbiol* 39:434–439.
9. Seki M, Iida K, Saito M, Nakayama H, Yoshida S (2004) Hydrogen peroxide production in *Streptococcus pyogenes*: Involvement of lactate oxidase and coupling with aerobic utilization of lactate. *J Bacteriol* 186:2046–2051.
10. Kreth J, Merritt J, Shi W, Qi F (2005) Competition and coexistence between *Streptococcus mutans* and *Streptococcus sanguinis* in the dental biofilm. *J Bacteriol* 187:7193–7203.
11. Bard AJ, Mirkin MV, eds. (2001) *Scanning Electrochemical Microscopy* (Marcel Dekker, New York), pp 1–15.
12. Wang X, Yang T, Feng Y, Jiao K, Li G (2009) A novel hydrogen peroxide biosensor based on the synergistic effect of gold-platinum alloy nanoparticles/polyaniline nanotube/chitosan nanocomposite membrane. *Electroanal* 21:819–825.

13. Mao L, Osborne PG, Yamamoto K, Kato T (2002) Continuous on-line measurement of cerebral hydrogen peroxide using enzyme-modified ring-disk plastic carbon film electrode. *Anal Chem* 74:3684–3689.
14. Liu X, Zweier LJ (2001) A real-time electrochemical technique for measurement of cellular hydrogen peroxide generation and consumption: Evaluation in human polymorphonuclear leukocytes. *Free Radical Biol Med* 31:894–901.
15. Horrocks BR, Schmidtke D, Heller A, Bard AJ (1993) Scanning electrochemical microscopy. 24. Enzyme ultramicroelectrodes for the measurement of hydrogenat surfaces. *Anal Chem* 65:3605–3614.
16. Wittstock G, Schuhmann W (1997) Formation and imaging of microscopic enzymatically active spots on an alkanethiolate covered gold electrode by scanning electrochemical microscopy. *Anal Chem* 69:5059–5066.
17. Wilhelm T, Wittstock G (2003) Analysis of interaction in patterned multienzyme layers by using scanning electrochemical microscopy. *Angew Chem Int Edit* 42:2248–2250.
18. Zhan D, Li X, Zhan W, Fan FF, Bard AJ (2007) Scanning electrochemical microscopy. 58. Application of a micropipet-supported ITIES tip to detect  $\text{Ag}^+$  and study its effect on fibroblast cells. *Anal Chem* 79:5225–5231.
19. Kirchner CN, Träuble M, Wittstock G (2010) Diffusion and reaction in microbead agglomerates. *Anal Chem* 82:2626–2635.
20. Li X, Bard AJ (2009) Scanning electrochemical microscopy of HeLa cells—Effects of ferrocene methanol and silver ion. *J Electroanal Chem* 628:35–42.
21. Cai C, Liu B, Mirkin MV, Frank HA, Rusling JF (2002) Scanning electrochemical microscopy of living cells. *Anal Chem* 74:114–119.
22. Liu B, Rotenberg SA, Mirkin MV (2000) Scanning electrochemical microscopy of living cells: Different redox reactivities of human breast cells and metastatic breast cancer cells. *Proc Natl Acad Sci USA* 97:9855–9860.
23. Fan FRF, Bard AJ (1999) Imaging of biological macromolecules on mica in humid air by scanning electrochemical microscopy. *Proc Natl Acad Sci USA* 96:14222–14227.
24. Zhan D, Fan FF, Bard AJ (2008) The Kv channel blocker 4-aminopyridine enhances  $\text{Ag}^+$  uptake: A scanning electrochemical microscopy study of single living cells. *Proc Natl Acad Sci USA* 105:12118–12122.
25. Anderl JN, Franklin MJ, Stewart PS (2000) Role of antibiotic penetration limitation in *Klebsiella pneumoniae* biofilm resistance to ampicillin and ciprofloxacin. *Antimicrob Agents Chemother* 44(7):1818–1824.
26. Bard AJ (1961) Effect of electrode configuration and transition time in solid electrode chronopotentiometry. *Anal Chem* 33:11–15.